Nuclear Instruments and Methods in Physics Research A 636 (2011) 61–66

Contents lists available at ScienceDirect

Nuclear Instruments and Methods in Physics Research A

journal homepage: www.elsevier.com/locate/nima

Monte Carlo modelling of gamma-ray stopping efficiencies of Geiger–Müller counters

I. Meric [a,d,*], G.A. Johansen [a,b,d], M.B. Holstad [c,d], R.P. Gardner [b]

[a] University of Bergen, Department of Physics and Technology, Allégaten 55, N-5007 Bergen, Norway
[b] Center for Engineering Applications of Radioisotopes, North Carolina State University, Raleigh, NC 27695-7909, USA
[c] CMR Instrumentation, Christian Michelsen Research AS, P.O. Box 6031, N-5892 Bergen, Norway
[d] The Michelsen Centre for Industrial Measurement Science and Technology, P.O. Box 6031, N-5892 Bergen, Norway

ARTICLE INFO

Article history:
Received 1 September 2010
Received in revised form
24 December 2010
Accepted 17 January 2011
Available online 1 February 2011

Keywords:
Geiger–Müller detector
Monte Carlo simulation
Gamma-ray stopping efficiency

ABSTRACT

A detailed study of the intrinsic stopping efficiency mechanisms of low energy gamma-rays (59.5 keV) in a Geiger–Müller counter is presented. MCNP5 and PENELOPE 2006 simulations have been carried out and the simulation results have been benchmarked with experimentally obtained stopping efficiencies. The results show that the inner wall interactions are critical for the gamma-ray stopping efficiencies.
© 2011 Elsevier B.V. All rights reserved.

1. Introduction

The Geiger–Müller tube (GMT) was introduced in 1928 and is still a popular radiation detector in applications where energy sensitivity is not required. Typical examples are exposure level and contamination measurements, and industrial process applications, such as density, level and thickness gauging. Its popularity is explained by the combination of ruggedness, simple operation and relatively low cost. There are GMT versions available for operation up to 200 °C, making the detector attractive for use in demanding environments like sub-sea systems and oil wells. Its downsides in many process applications are limitations in gamma-ray stopping efficiency ($\sim$1%), count-rate capability ($\sim 10^4$ counts/s) and in some cases also the life time ($\sim 10^{10}$ counts). The objective of this work has been to develop and benchmark a Monte Carlo (MC) model of a GMT. Such a model is an efficient tool in identifying and understanding critical parameters in the gamma-ray stopping efficiency.

2. Geiger–Müller tube

The Centronic ZP1200 GMT was picked for this study. This is a versatile and robust GMT with many applications, such as in the Tracerco Profiler™, which is a multiple source/detector system for measurement of component phase heights in gas/oil/water gravity separators [1,2]. The applied radioisotope is ^{241}Am with principal emission gamma-ray energy at 59.5 keV. The ZP1200, which is shown in Fig. 1, is used for this application even though it does not have a low attenuation radiation entrance window. This is because such a window would make the tube more susceptible to damage and failure in harsh environments.

To make charge multiplication possible at relatively low bias voltages [5], the pressure of the fill gas in the ZP1200 is only about 135 mbar as in many similar tubes. This means that the absorption of gamma-rays in the fill gas is negligible. Virtually all counts at the GMT output are generated by avalanches from secondary electrons, such as photoelectrons and Compton recoil electrons, with sufficient energy to reach the fill gas from gamma-ray interactions in the solid parts of the GMT. The gamma-ray stopping efficiency of the tube thus depends on the stopping properties of the solid parts, mainly the cathode wall, and the efficiency by which the secondary electrons can reach the fill gas. The latter is a function of the electrons' emission position and energy, and their energy loss per unit path length, i.e. the stopping power ($-dE/dx$) in the material. The stopping power describes the mean energy loss of electrons of certain energy in a given material and does not take into account the fluctuations about this value, i.e. the so-called energy straggling [6]. In the Continuously Slowing Down Approximation (CSDA), the mean electron range, R, is given as the maximum track length an electron can traverse before losing all its energy and being absorbed by the medium. The escape length of an electron will therefore depend on its emission position in the solid parts of the GMT, i.e. how close to or how far from the structure/fill gas interfaces the electron is emitted, as well as on its average range

* Corresponding author at: University of Bergen, Department of Physics and Technology, Allégaten 55, N-5007 Bergen, Norway.
E-mail address: ilker.meric@ift.uib.no (I. Meric).

0168-9002/$ - see front matter © 2011 Elsevier B.V. All rights reserved.
doi:10.1016/j.nima.2011.01.083

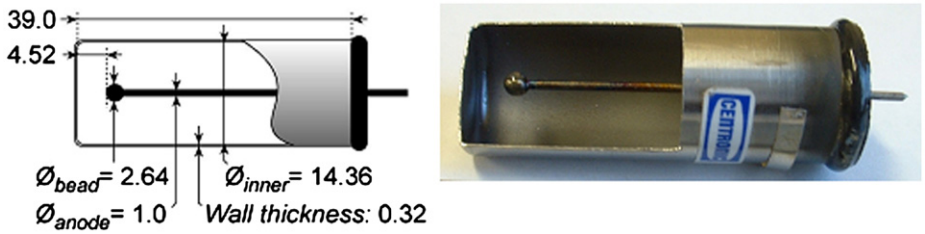

Fig. 1. Cross-sectional view of the ZP1200 GMT used for the study. All dimensions are in mm [3,4].

which, in turn, is dependant on the physical properties of the medium and the initial electron energy. An analytical method for estimating the GMT stopping efficiency has been presented and applied for a limited number of tube configurations [7], so has the Monte Carlo methods [8] but in both cases with focus on gamma-ray energies above 100 keV.

3. Experiment

The geometry of the experimental system [9] is shown in Fig. 2: An X.101 encapsulated 14 mCi ^{241}Am point source was installed in a cone beam lead collimator and three additional plate collimators, each 1 mm thick and with 3 mm diameters holes, were positioned as shown between this and the detector surface. For all experiments a $10\times10\times2$ mm^3 CdZnTe semiconductor detector was used as reference to measure the beam intensity incident on the GMT front surface. The CdZnTe detector was biased to 180 V by a Tennelec TC954 high voltage supply and the signals were read-out and counted with an eVProducts eV550/A2968 preamplifier, a Tennelec TC 241 main amplifier and a PC-controlled Tennelec TC512 counter. To correct the small transmission leakage in the CdZnTe detector and the attenuation in its 1 mm thick Al front window, the measured intensity was multiplied by 1.0718 to provide the reference intensity. This number was found using MC simulation. The counting or integration time for all reference measurements was 300 s, with a count-rate of about 18 kc/s. This means the statistical error in the reference measurements can be neglected. A NE PSR8 scaler/rate metre was used to provide the 500 V bias for the GMT and to count its anode output pulses.

The experiment described in Fig. 2 was repeated several times with different casings covering the GMT as shown by the dashed lines in the figure. This was done to study the effect of scattered radiation as well as the effect of X-ray fluorescence on the total intrinsic stopping efficiency of the GMT. Two tube materials, aluminium and tin, were chosen. Aluminium was chosen because it has relatively low Z-number and Compton scattering as the dominant interaction mechanism at 59.5 keV, and tin because of its K-edge at 29.2 keV and its relatively lower photon attenuation compared to other metals. The low photon attenuation will reduce the photon absorption in the metal casing, and thus increase the flux of photons on the GMT cathode walls which, in turn, might produce secondary electrons with sufficient energy to reach the fill gas and contribute to the overall stopping efficiency of the counter. A few combinations of tube lengths (l) and thicknesses (t) were also investigated.

4. MC model

It is generally demanding to make accurate MC models of gas detectors; however, the requirements are more relaxed in the "binary" GMT case where only the number of electrons entering

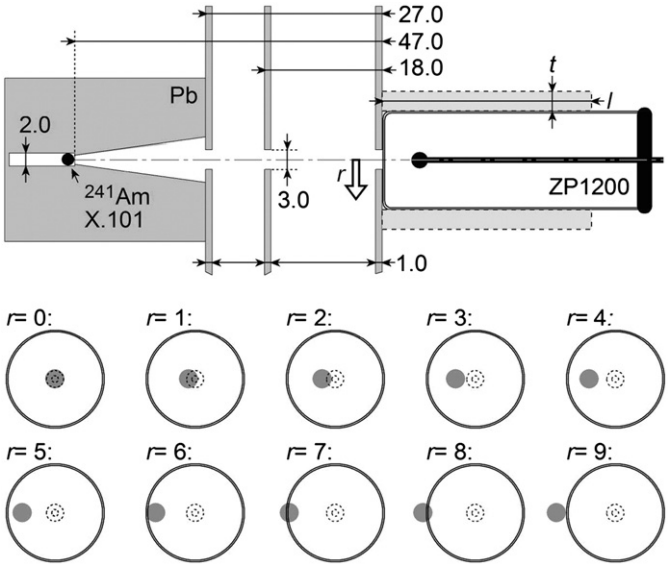

Fig. 2. Measurement geometry used for the experiments and the simulations. The tube was moved radially in steps from $r=0$ to $r=9$ mm as indicated below where the shaded circle is the beam and the dashed circles are the anode and its tip bead, respectively. All dimensions are given in mm.

the fill gas needs to be considered. There is no need to know the energy or entrance positions of each electron accurately, neither are the charge multiplication properties significant. This development is based on illumination of the tube from the front with a 3 mm diameter beam at different radial positions. By moving the beam centre in steps of 1 mm from $r=0$ mm, which is along the anode wire, towards $r=9$ mm it is possible to monitor the contributions from the different parts of the GMT to the total response, which in all cases should match the experimental values.

A model of the ZP1200 and the measurement geometry shown in Fig. 2 was developed in two different general purpose MC codes, MCNP5 and PENELOPE. In both codes, the model was implemented using gamma-ray and electron transport mode, but, in the MCNP5 model, in order to reduce the computational time, a variance reduction technique called range rejection was applied to the electron transport. This was done by simulating electron transport only in the inner 50 μm of all surfaces surrounding the fill gas. This is beyond the maximum range of secondary electrons created by 59.5 keV gamma-rays in these materials.

It soon became evident that accurate geometry and material specification were crucial for this problem. The material composition listed in Table 1 is based on an analysis carried out and provided by Centronic, whereas a tube was cut open to verify the dimensions as specified in Fig. 1. The cathode wall and the anode pin are both iron chromium (FeCr) alloys, and in addition the cathode has a coating of 5–8 μm so-called grey chromium (Cr) that is plated onto the inner wall.

Table 1
Composition of the GMT materials [10].Z_{eff} ($m=4.5$). Z_{eff} is the effective atomic number [5].

Material	Element	Weight percent (%)	Density (g/cm^3)	Z_{eff}
Cathode	Fe	70.18	7.55	25.94
	Cr	28.47		
	Si	0.47		
	Mn	0.37		
	Ni	0.18		
	V	0.08		
	Others	0.25		
Anode	Fe	69.4	7.40	25.88
	Cr	28.4		
	Si	1.40		
	Others	0.8		
Anode tip and back wall	Si	56.05	2.47	11.97
	Pb	29.8		
	Na	7.7		
	K	4.5		
	Al	1.4		
	Others	0.55		
Fill gas	Ne	99.403	0.0001	10.12
	Ar	0.1		
	Br	0.498		

In the MCNP5 model, three different output tallies were used to calculate the gamma-ray stopping efficiency of the tube and its different contributions. The first is a current tally (f1) recording the number of gamma photons entering through the opening of the plate collimator into the front of the detector. This number is independent of the beam position. This tally had to be made directional so that the current could be determined without backscattered events. The reason for this is that the surface current tally in MCNP5 will yield the total number of particles, i.e. both transmitted and backscattered, crossing a surface when cosine binning is not used. Using cosine binning in conjunction with the surface current tallies will make sure that the net current in each direction relative to the source will be provided in the output. The second, which is also a current tally, gives the numbers of electrons entering the fill gas volume through (a) the front surface of the cathode, (b) the side surface of the cathode, (c) the back glass wall, (d) the anode wire and finally (e) the anode tip glass bead. These current tallies need not to be defined in conjunction with the cosine binning option as the transport of all secondary electrons is terminated immediately after entering the cell defined by the fill gas. The assumption is then that all secondary electrons entering the fill gas give rise to a count pulse on the GMT output. The number of counts is thus equal to the sum of all electron current contributions from the different surfaces when one correction is made: There are a few occasions where each initial gamma-ray interaction produces more than one electron that reaches the gas, for instance one photoelectron and one Auger electron or multiple Compton recoil electrons. These should only be registered as one count. To correct this a third, so-called pulse height tally (f8) is used for the cell defined by the fill gas volume. The f1, i.e. the surface current tally, and the f8, i.e. the pulse height tally, are explained in detail in the MCNP5 user's manual [11]. The f8 tally is used to model a real detector in a given cell and provides all energy deposition in the fill gas originating from one and the same initial gamma-ray interaction in one event, and will thus yield the correct number of counts. Since electron transport is not simulated in the fill gas cell, the full energy of these electrons is recorded once they enter the cell.

The same model was also implemented in PENELOPE version 2006 using the quadric geometry package PENGEOM. Previously mentioned assumptions and corrections apply also to the PENELOPE model of ZP1200. The only significant differences were the programming effort required by the PENELOPE code and the fact that the range rejection for electrons was not considered. The main programme penmain.f was modified according to the requirements of the system to be modelled. User-defined counters were used to count the number of electrons crossing the fill gas/structure interfaces. Each secondary electron created during the course of the simulations was flagged by the history number and terminated as soon as they entered the region defined by the fill gas so as to avoid double counting as well as avoiding multiple counts from the same history.

Some differences between the MCNP5 calculated GMT intrinsic stopping efficiencies and those calculated using PENELOPE 2006 were to be expected. This is mainly due to the fact that MCNP5 utilises the so-called condensed history (CH) scheme for electron transport in which the electron trajectory is divided into several energy-steps which, in turn, are divided into sub-steps. The energy loss of electrons is sampled at the beginning of each energy-step and the angular deflections are sampled at the end of each sub-step from appropriate multiple scattering energy loss and angular distributions, respectively. On the other hand, PENELOPE is capable of utilising the mixed simulation scheme in which hard events, i.e. collisions where the electron energy loss is greater than a preset energy threshold and the angular deflection is greater than a corresponding angular deflection threshold, are simulated in detail whereas the soft collisions, i.e. collisions that do not cause large angular deflections or energy losses, are simulated using the CH technique [11,12]. This means that PENELOPE and MCNP5 employ similar electron transport schemes below the preset threshold values. In order to avoid inaccuracies, the pertinent simulation parameters, C1, C2, WCC and WCR [12] were all set equal to zero in the PENELOPE model to enable detailed electron simulation.

5. Results and discussions

The results of the experiments and of the MC simulations are presented in Fig. 3, where the intrinsic stopping efficiency is determined as the ratio of the number of detected events in the GMT to the number of incident gamma photons through the opening of the collimator closest to the GMT.

The large variations in the experimental results shown in Fig. 3 can be explained by repeatability mounting or positioning of the source and the GMT. Simulation results show that there is a strong sensitivity to misalignment of the GMT of just $\pm 0.5^\circ$ to the incident beam, particularly at the position ($r=5$ mm) along the inner wall of the tube (see the error bar in Fig. 3).

The most obvious comment on the results is the deviation between the measured intrinsic stopping efficiency and the prediction from the simulations. The first is more than twice the latter. It can also be observed that the results from PENELOPE and MCNP5 agree well except for negligible differences.

Moreover, an attempt was made to model the GMT using the latest version of PENELOPE, PENELOPE 2008. The electron physics is essentially unchanged when compared to the previous version of the code [13]. Thus, it was expected that the results from the two versions of the code would be the same. This was confirmed through implementation of the GMT model in PENELOPE 2008.

The simulated effects of covering the GMT with tubes also need some comments. This is done in order to investigate the possible effects of increased scatter into the detector surfaces and thereby to study whether or not this would increase the stopping

efficiency of the detector. From the MC results and at the same time keeping in mind the sensitivity of the detector to its positioning with respect to the incident photon beam, it can be concluded that the overall effect of surrounding the detector with tubes is only marginal.

Further research revealed that the reason for the underestimation was twofold for each MC model: At this energy (59.5 keV) the simulations predict that 90% of the electrons reaching the fill gas and contributing to the signal is generated by interactions 5 μm or closer to the inner surface of the tube. For the cathode this could mean that the real probability for the secondary electrons to reach the fill gas with sufficient energy is greater than the simulated one because of the porous structure of the plated Cr layer. The porous structure of this layer increases the inner surface area of the cathode wall and thus increases the probability for the secondary electrons to penetrate into the fill gas and cause a discharge. In order to be able to take into account the surface porosity, saw tooth surfaces were implemented on the inner front wall. The teeth dimensions were varied in order to study the effects of increased inner wall surface area on the intrinsic stopping efficiency of the GMT.

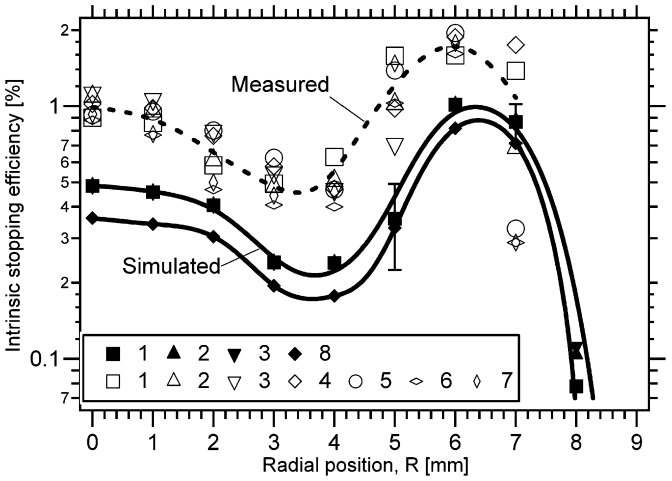

Fig. 3. Simulated (solid legends and best fit curve) and experimental (open legends and dashed best fit curve) intrinsic stopping efficiency as a function of radial position of axis of the beam with 3 mm diameter. The numbers next to the legends represent: (1) Bare GMT measured and simulated using MCNP5, (8) Bare GMT simulated using PENELOPE and further GMT surrounded by tubes of the following material and dimensions ($l \times t$ in mm): (2) Al (15×3), (3) Al (32×3), (4) Al (15×3) with cone opening, (5) Al (15×9), (6) Sn (15×5), and (7) Sn (15×2). Case 4 is similar to case 2 except that the covering tube has a cone inner opening in the front. The error bars shown on the simulation results of the bare GMT is the effect of tilting the beam $\pm 0.5^{\circ}$ to the GMT anode axis.

PENELOPE simulations using saw tooth surfaces on the inner front wall have confirmed the above observation and the results are presented in Fig. 4 for different saw tooth dimensions. Obviously, the increased inner surface of the front wall leads to an increase in the number of secondary electrons that penetrate into the fill gas due to shorter distances that have to be traversed by the low energy secondary electrons. The same behaviour was observed also in the MCNP5 model of the detector.

Furthermore, it was decided to take into account the porosity of the Cr-coating in a new MC model and run a new set of simulations. It soon became evident that the implementation of a saw tooth surface is a very inefficient way of accomplishing this task as the number of surfaces required increases rapidly. This, in turn, leads to a significant increase in the required simulation time as well as the fact that the total number of surfaces allowed by both MCNP5 and PENELOPE would quickly be exhausted when the surface porosity of the side walls is also taken into account. One important observation is that the implementation of the porous Cr-coating has no significant effect on the photon transport through this layer. This was confirmed by MC simulations by tallying the total number of photons absorbed in this layer where this number was the same for both the smooth Cr-coating and the porous Cr-coating. This means that one could consider using a smooth Cr-coating in which the material density, i.e. Cr density, can be reduced by a factor as soon as a secondary electron is created in this volume. In a different work, a similar approach was considered for simulating electron channelling effects in sodium iodide (NaI) scintillation detector [14]. In PENELOPE it is possible to achieve this without having to modify the source code, thus PENELOPE was used for the final experiment.

To find the best density multiplication factor, the comparison between the simulated and the experimental results was based on a chi-square test of distributions [15]. To accomplish this, the density of the Cr-coating was gradually altered. A chi-square test was so conducted to study whether or not the simulations modelled the GMT well. To conduct the chi-square test, the count rates were used rather than the stopping efficiencies. Since this is a counting experiment, the standard deviations of the experimental results at each radial position were set equal to the square root of the count rates. The stopping efficiency curves obtained for a bare GMT for different density multiplication factors are

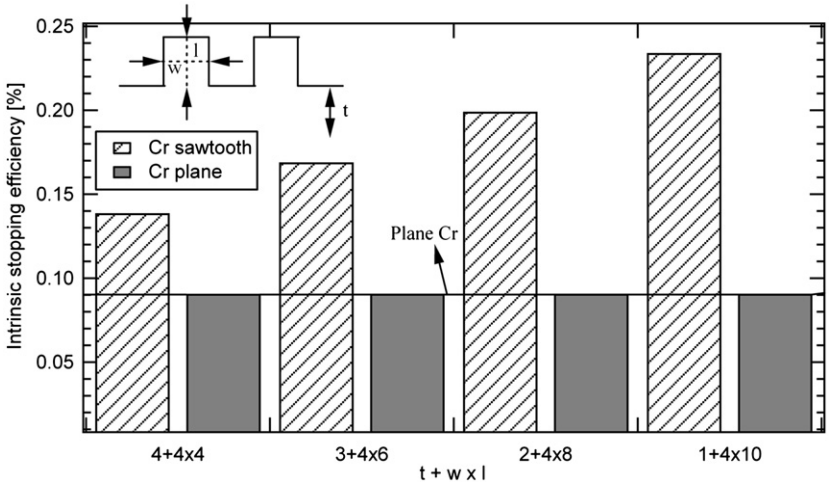

Fig. 4. Simulated contribution of the front cathode wall to the total intrinsic stopping efficiency of the ZP1200 tube when saw tooth surfaces are used on the inner front wall, thus increasing the inner surface area. *t*: thickness of the flat part of the coating, *w*: tooth width and *l*: tooth height . All dimensions are in μm.

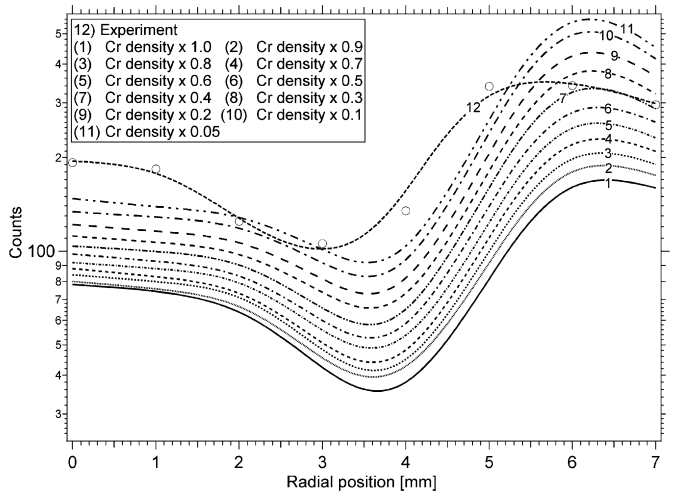

Fig. 5. Simulated stopping efficiencies for several density multiplication factors (best fit lines from (1) to (11)), ranging from 1.0 to 0.05, using PENELOPE and experimental (open legends and the dashed best fit curve, (12)) stopping efficiencies of the ZP1200 GMT as a function of the radial beam position relative to the centre of the detector.

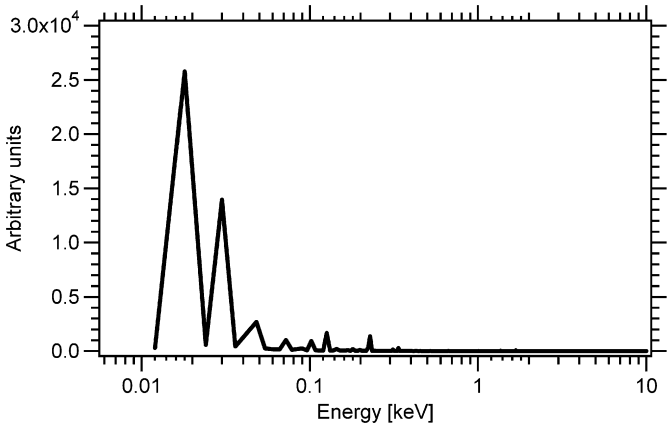

Fig. 6. Energy loss of electrons in single inelastic collisions recorded for the entire detector using PENELOPE.

presented in Fig. 5 along with the experimental curve obtained for a bare GMT. The reduced chi-square value for each of these cases was so determined according to the following equation [15]:

$$\chi^2_\nu = \frac{1}{\nu}\sum_{i=1}^{8}\frac{\left(\varepsilon_i^{\mathrm{sim}}-\varepsilon_i^{\mathrm{exp}}\right)^2}{\left(\sigma_i^{\mathrm{exp}}\right)^2} \quad (1)$$

where ν is the degree of freedom, $\varepsilon_i^{\mathrm{sim}}$ is the count-rate obtained through MC simulations, $\varepsilon_i^{\mathrm{exp}}$ is the experimentally obtained count rates and σ_i^{exp} is the standard deviations of the experimental results obtained at each radial position. The reduced chi-square reached its minimum value for a density multiplication factor of between 0.4 and 0.3 where a reduced chi-square value of 41.62 was obtained. Generally, a reduced chi-square value of about 1.0 is indicative of a good description of an experimental distribution. In this case, the mismatch among the experimental and simulated curves leads to a high reduced chi-square value, and thus indicate the fact that other parameters than only the porous structure of the Cr-coating, such as sensitivity to positioning and repeatability, should be considered.

In case of PENELOPE, the second pertinent mechanism that might contribute to the underestimation is the treatment of electron inelastic collisions. PENELOPE treats inelastic collisions of electrons using the Generalised Oscillator Strength (GOS) model, details of which can be found in Ref. [12]. In this model, the contributions from the outer atomic shells are basically grouped into a single delta-oscillator with a given resonance energy, thus disregarding the detailed treatment of the contributions of the individual outer atomic shells.

The energy loss of electrons in single inelastic collisions was recorded for the entire detector. The effects of the GOS model can readily be seen in Fig. 6, where no energy loss below 12 eV is recorded. The anode bead and the back wall of the tube consist mostly of Si and Pb (see Table 1). The outermost shell of lead is the P3 shell with binding energy of 5.29 eV. This means that energy losses of the order of 5.29 eV would physically be possible. The fact that this is not treated explicitly in the PENELOPE model might have an impact on the spatial distribution of the secondary electrons. In MCNP5, however, the treatment of charged particle transport is fundamentally different than that of PENELOPE. As mentioned before, MCNP5 employs the CH technique for the transport of charged particles in which no single collisions are treated in detail. Each major electron step is further broken into several sub-steps, the number of which depends only on the material properties. The electron energy loss rate is sampled at the beginning of each major step while the angular deflections are continuously updated at the end of each sub-step. Moreover, the particle path between the start and end points of the sub-step is approximated as a straight line. This might, in turn, lead to a slight distortion in the electron spatial distributions within the solid parts of the GMT. It is, however, believed that the physics of electron transport in both PENELOPE 2006 and MCNP5 would be nothing more than a minor cause of the underestimated intrinsic stopping efficiencies. It is believed that the major cause, at 59.5 keV, is the fact that the Cr-coating is plated onto the inner cathode walls of the tube and that the coating has a porous structure rather than having a perfectly smooth surface. To the best of the authors' knowledge, no experimental data that could confirm such a hypothesis have yet been published. However, the MC simulations indicate that the increased surface area of the Cr-coating on the inner cathode walls will lead to a significant increase in the contribution from these surfaces when the primary photon energy, and through that the electron energy, is low. This might be explained as a direct consequence of the fact that a fraction of electrons will traverse much shorter distances before crossing wall/gas interfaces and cause a discharge.

6. Conclusions and future work

MC models of a ZP1200 GMT were developed using two different general purpose codes, MCNP5 and PENELOPE 2006. It was observed that both the MC models have underestimated the intrinsic gamma-ray stopping efficiencies of the GMT. The mechanisms that might be responsible for the underestimation have been investigated. The porosity of the Cr-coating that is plated onto the inner surface of the cathode walls was identified as the major responsible mechanism for the underestimation in both models. Utilising PENELOPE 2006, new simulations were run taking into account the porosity of the Cr layer. The simulations were repeated for various density multiplication factors ranging from 1.0 to 0.05. The change in the simulated stopping efficiencies confirms the above observation. However, upon comparison between the simulated and the experimental results, a minimum reduced chi-square value of 41.62 was obtained indicating the fact that other parameters such as the repeatability in the experiments and the sensitivity of the detector to beam positioning should also be taken into account. For more accurate MC modelling, the possible effects of PENELOPE treatment of the electron inelastic collisions on the simulated intrinsic stopping

efficiencies of the GMT must be checked against a single scatter MC code in which all of the microscopic interactions of electrons are simulated individually. It is believed that, for modelling GM counters, a microscopic, specific-purpose MC code would be more suitable to study the different physical mechanisms of intrinsic stopping efficiencies of GMTs as this type of MC code will not introduce any approximations in the treatment of electron transport. The future work will therefore involve developing a single scatter MC code capable of simulating photon/electron cascades for this purpose.

Acknowledgements

The authors acknowledge provision of ZP1200 tubes and data from Mike Bates and Marc Abilama in Centronic and discussions with Peter Jackson in Tracerco. Support on Monte Carlo simulation by the CEAR members at North Carolina State University, in particular PhD students Cody Peeples and Jiaxin Wang, and Xiaogang Han at Baker Atlas is also very much appreciated.

References

[1] B.T. Hjertaker, G.A. Johansen, P. Jackson, J. Electron. Imaging 10 (2001) 679.
[2] R.P. Lee, Meas. Control 35 (2002).
[3] Centronic, Databook on Geiger Müller Tubes, Centronic, Croydon, UK. 〈http://www.centronic.co.uk/tube_theory.htm〉.
[4] P. Jackson, Personal communication, Tracerco, Cleveland, UK, 2006.
[5] G.A. Johansen, P. Jackson, The Geiger-Müller Tube, Radioisotope Gauges for Industrial Process Measurements, John Wiley & Sons Ltd, Wiltshire, UK, 2004, p. 313.
[6] N.J. Carron, An Introduction to the Passage of Energetic Particles through Matter, CRC Press Taylor & Francis Group, Boca Raton, Florida, 2007.
[7] T. Watanabe, Nucl. Instr. and Meth. A 438 (1999) 439.
[8] W.L. Dunn, R.P. Gardner, Nucl. Instr. and Meth. A 103 (1972) 373.
[9] M.B. Holstad, Implementation of Dual Mode Gamma-ray Densitometer for Gas Fraction Measurement in Multiphase Pipe Flows, M.Sc. Thesis, Bergen, Norway, 2000.
[10] M. Bates, M. Abilama, Personal communication, Centronic, Croydon, UK, 2010.
[11] X-5, Monte, Carlo, Team, A General Monte Carlo N-Particle Transport Code, Version 5, Los Alamos National Laboratory, Los Alamos, USA, 2003. 〈http://mcnp-green.lanl.gov/manual.html〉.
[12] F. Salvat, J.M. Fernandez-Varea, J. Sempau, PENELOPE 2006: A Code System for Monte Carlo Simulation of Electron and Photon Transport, OECD, France, 2006. 〈http://www.nea.fr/science/pubs/2006/nea6222-penelope.pdf〉.
[13] F. Salvat, J.M. Fernandez-Varea, J. Sempau, PENELOPE 2008: A Code System for Monte Carlo Simulation of Electron and Photon Transport, OECD, France, 2008. 〈http://www.nea.fr/science/pubs/2009/nea6416-penelope.pdf〉.
[14] A. Sood, R.P. Gardner, Nucl. Instr. and Meth. B 213 (2004) 100.
[15] P.R. Bevington, D.K. Robinson, Data Reduction and Error Analysis for the Physical Sciences, McGraw-Hill, New York, NY, 2003.